Continental-scale patterns of extracellular enzyme activity in the subsoil: an overlooked reservoir of microbial activity

Nicholas Dove[1], Keshav Arogyaswamy[2], Sharon Billings[3], Jon Bothoff[2], Chelsea Carey[4], Caitlin Cisco[5], Jared DeForest[6], Dawson Fairbanks[7], Noah Fierer[8], Rachel Gallery[7], Jason Kaye[9], Kathleen Lohse[10], Mia Maltz[2], Emilio Mayorga[11], Jennifer Pett-Ridge[12], Wendy Yang[5], Stephen Hart[13], and Emma Aronson[2]

[1]Oak Ridge National Laboratory
[2]University of California Riverside
[3]University of Kansas
[4]Point Blue Conservation Science
[5]University of Illinois at Urbana-Champaign
[6]Ohio University
[7]University of Arizona
[8]University of Colorado Boulder
[9]The Pennsylvania State University
[10]Idaho State University
[11]University of Washington
[12]Lawrence Livermore National Laboratory
[13]University of California Merced

May 5, 2020

Abstract

Stabilization of microbial-derived products such as extracellular enzymes (EE) has gained attention as a possibly important mechanism leading to the persistence of soil organic carbon (SOC). While the controls on EE activities and their stabilization in the surface soil are reasonably well-understood, how these activities change with soil depth and possibly diverge from those at the soil surface due to distinct physical, chemical, and biotic conditions remains unclear. We assessed EE activity to a depth of 1 m (10 cm increments) in 19 soil profiles across the Critical Zone Observatory Network, which represents a wide range of climates, soil orders, and vegetation types. Activities of four carbon (C)-acquiring enzymes (α-glucosidase, β-glucosidase, β-xylosidase, and cellobiohydrolase), two nitrogen (N)-acquiring enzymes (N-acetylglucosaminidase and leucine aminopeptidase), and one phosphorus (P)-acquiring enzyme (acid phosphatase) were measured fluorometrically along with SOC, total N, Olsen P, pH, clay concentration, and phospholipid fatty acids, which we used to characterize the microbial community composition and biomass (MB). For all EEs, activities per gram soil correlated positively with MB and SOC; all of which decreased logarithmically with depth ($p < 0.05$). Across all sites, over half of the potential soil EE activities per gram soil consistently occurred below 20 cm for all measured EEs. Activities per unit MB or SOC were substantially higher at depth (soils below 20 cm accounted for 80% of whole-profile EE activity), suggesting an accumulation of stabilized (i.e., mineral sorbed) EEs in subsoil horizons. The pronounced enzyme stabilization in subsurface horizons was corroborated by mixed-effects models that showed a significant, positive relationship between clay concentration and MB-normalized EE activities in the subsoil. Furthermore, the negative relationships between soil C, N, and P and C-, N-, and P-acquiring EEs found in the surface soil decoupled at 20 cm, which could have also been caused by EE stabilization. This suggesting that EEs do not reflect soil nutrient availabilities at depth. Taken together, our results suggest that deeper soil horizons hold a significant reservoir of EEs, and that the controls of subsoil

EEs differ from their surface soil counterparts.

INTRODUCTION

Globally, soils store approximately 1,500 Pg of soil organic carbon (SOC) in the upper meter of the soil profile, with 50-67% of SOC occurring below 20 cm (Jobbágy & Jackson 2000). The persistence of this C pool is in part controlled by extracellular enzymes (EEs) primarily released by soil microorganisms that decompose soil organic matter (Burns *et al.* 2013). However, even though the majority of SOC occurs in the subsoil, most studies of soil microorganisms and the EEs they secrete focus on the upper soil layers. While the age (and thus persistence) of SOC increases with depth (Trumbore *et al.* 1996; Paul *et al.* 1997; Rumpel *et al.* 2002), recent studies have shown that subsoil (>20 cm depth) C is still vulnerable to decomposition. Indeed, subsurface microbial communities have resource demands that rival those of surface soils when normalized to a microbial biomass (MB) basis (Jones *et al.* 2018). Understanding subsurface processes is critical in an age of global change because vulnerability of SOC to EE attack could be enhanced by increased temperatures or wetting/drying cycles (Schimel *et al.* 2011; Hicks Pries *et al.* 2017). This means that if subsoils are disturbed (either physically or through altered environmental conditions), portions of the soil organic matter pool at depth could become accessible to EEs, resulting in the mineralization of significant quantities of C and nutrients. Therefore, increased understanding of EE patterns at depth could help elucidate the mechanisms of subsoil organic matter decomposition and aid in predicting how pools of SOC and nutrients will be affected by ongoing global change factors.

Because EEs both respond to and influence soil properties, the study of EEs has led to greater insights into soil C persistence (Billings & Ballantyne 2013; Birge *et al.* 2015; Dove *et al.* 2019), nitrogen (N) and phosphorus (P) mineralization (Weintraub & Schimel 2003; Waring *et al.* 2014; Chen *et al.* 2018), ecosystem development (Olander & Vitousek 2000; Selmants & Hart 2010; Turner *et al.* 2014), and microbial metabolism (Sinsabaugh & Shah 2011, 2012; Sinsabaugh *et al.* 2013). Given that the methods for measuring EE activity in soils are relatively high-throughput, inexpensive, and reproducible across laboratories (Dick *et al.*2018), it is one of the most common soil biogeochemical measurements ('Soil extracellular enzyme activity' resulted in 2,013 records using Clarivate Analytics Web of Science as of Jan. 28, 2020). However, despite the widespread measurement of soil EEs, most studies have focused on EE activities in surface horizons, with few studies exploring EE activity patterns in soil horizons below 20 cm (but see Taylor *et al.* 2002; Kramer *et al.* 2013; Stone *et al.* 2014; Taş *et al.* 2014; Schnecker *et al.* 2015; Loeppmann *et al.* 2016; Jing *et al.* 2017).

Numerous soil physical and biogeochemical properties change with depth. As organic matter (both SOC and organically bound nutrients) moves into the subsoil, it becomes increasingly more microbially processed and sorbed onto charged mineral surfaces (Rumpel & Kögel-Knabner 2010), which concomitantly increase with depth. Soil pH may also increase with depth in instances where the parent material is enriched in base cations (Brubaker *et al.* 1993). These gradients in soil properties result in subsoil microbial communities that are vastly different than their surface soil counterparts (Eilers *et al.* 2012; Brewer *et al.* 2019). Soil pH (Sinsabaugh *et al.* 2008; Kivlin & Treseder 2014), substrate availability and demand (Olander & Vitousek 2000; Dove *et al.* 2019), and microbial community composition (Schnecker *et al.* 2015) influence EE activities in surface soils. Because these factors change along soil profiles, EE activities should also change with soil depth. Two main generalizations have emerged from the few studies that have investigated EE activities in subsoils: 1) EE activities decline with depth in association with decreases in soil organic matter concentrations and decreases in microbial biomass (Taylor *et al.* 2002; Stone *et al.* 2014; Loeppmann *et al.*2016), and 2) EE activities at depth are less responsive to surface conditions, manipulations, and management practices (Kramer *et al.* 2013; Jing *et al.* 2017; Yao *et al.* 2019). However, our ability to quantify the total EE pool and elucidate the controls on EEs in subsoils has been hindered by unstandardized ancillary measurements, assay parameters, and depths of sampling across studies (Nannipieri *et al.* 2018).

Systematic, continental- and global-scale assessments and meta-analyses of EEs in surface soils have begun to clarify controls and correlates of EE activity (Sinsabaugh *et al.* 2008, 2009; Xiao *et al.*2018). For instance,

EE stoichiometry (the ratio of C-, N-, and P-acquiring enzymes), which can represent the relative C, N, and P demand (Sinsabaugh & Shah 2012), scales at 1:1:1 (C:N:P) globally across soil, freshwater, and saltwater ecosystems, suggesting that the plasticity of microbial resource demand is somewhat constrained (Sinsabaugh *et al.* 2008, 2009). These large-scale assessments also confirm that pH, substrate availability, and microbial demand influence EE activity in surface soils (Sinsabaugh *et al.* 2008, 2009; Xiao *et al.* 2018). However, it is currently unknown if these controls in surface soils extend into the subsoil. We posit that EE activities at depth may follow different patterns than in the surface horizons given that EEs at depth are less responsive to environmental perturbations (Jing *et al.* 2017), subsoils have greater heterogeneity of organic substrates than at the surface (Salomé *et al.* 2010), and the microbial communities at depth are dominated by oligotrophic microorganisms (Brewer *et al.* 2019).

To quantify EE activities and elucidate their controls throughout the soil profile, we sampled the upper meter of mineral soil at 10 cm increments in 19 soil pits across the 10 United States National Science Foundation-supported Critical Zone Observatories (CZOs) in the United States of America (USA). We hypothesized that EE activities per gram (g) soil would decline with depth due to decreased SOC and MB concentrations; however, a significant proportion of EE activity in the top meter of soil would occur below 20 cm depth. We also hypothesized that the fundamental controls on EE activities would differ between surface and subsoil horizons due to shifting biological, chemical, and physical conditions throughout the soil profile. Specifically, as organically bound microbial resources decrease with depth, mineral sorption of both substrates and EEs will become a more dominant control of potential EE activity. Our overall goal was to quantify potential EE activity in the subsoil over a diverse set of soils, ecosystems, and climates to elucidate how EE activity mediates subsoil C and limiting nutrient availabilities in order to improve predictive understanding.

METHODS

Site selection and sampling

Samples were collected from the network of 10 Critical Zone Observatories (CZOs, http://criticalzone.org) across the USA, which represents a wide range of hydrogeological provinces, soil orders, and vegetation types as described in Brewer et al. (2018). Soils were collected at peak greenness (as estimated from NASA's MODIS: MODerate-resolution Imaging Spectroradiometer) between April 2016 and November 2016, with the exception of the Eel River CZO samples, which were collected in May 2017 (also at peak-greenness). At each CZO, we excavated two separate soil profiles ("sites") selected to represent distinct soil types and landscape positions (Table 1). Any organic horizon was first removed, and then mineral soils were sampled in 10-cm increments with a sterile hand trowel dug into the face of each soil pit to a depth of at least 100 cm or to refusal.

All soil samples were shipped overnight at 4 °C to the University of California, Riverside for processing. A portion of each field sample was sieved (< 2 mm), homogenized, divided into subsamples for further analyses, and frozen (-20 degC). For some soils (particularly some wet, finely textured depth intervals), sieving was impractical. These samples were homogenized and larger root and rock fragments were removed by hand. In addition, as samples from SHAL (70-100 cm depth; see Table 1 for site abbreviations) consisted almost entirely of medium-sized weathered bedrock (Cr material), soil was collected by manually crushing weathered bedrock with a ceramic mortar and pestle with this material then passed through a 2-mm sieve.

Soil physiochemical measurements

Soil pH, gravimetric water content, and clay concentration were measured using modified Long-Term Ecological Research (LTER) protocols (Robertson*et al.* 1999). Briefly, soil pH was determined in a 1:1 (weight to volume) solution using 15 g of field-moist soil and 15 ml of Milli-Q water (Millipore Sigma, Burlington, MA, USA). The solution was measured on a Hannah Instruments (HI; Woonsocket, RI, USA) 3220 pH meter equipped with a HI 1053B combination glass pH electrode, designed for use with solid suspensions. For determining gravimetric water content, approximately 7 g field-moist soil was dried at 105 oC for a minimum of 24 h. Soil texture was measured on oven-dried and sieved soil using the hydrometer method following Gee & Bauder (2018).

Prior to soil total organic C and N analysis, soils were freeze-dried using a Savant Novalyphe-NL500 freezer dryer (Savant, Farmingdale, NY, USA) and ground to a fine powder using a roller mill. If effervescence occurred when a drop of 1 M HCl was added to a subsample of each soil sample, then inorganic C was removed from 2 g of the soil sample by twice-washing with 30 mL 0.1 N HCl (allowing the soil slurry to stand for 1 h during each wash), twice-washing with 30 mL DI, and then freeze-dried. The soil samples were analyzed for total organic C and total N by continuous-flow, direct combustion using a Vario Micro Cube elemental analyzer (Elementar, Hanau, Germany).

Microbially available orthophosphate, referred hereafter as Olsen P, was estimated by extracting 1 g of soil with 200 ml of 0.5 M $NaHCO_3$ at pH 8.5 (Olsen *et al.* 1954). Briefly, slurries were shaken for 30 min and filtered through Whatman No. 42 filters. Orthophosphate was measured colormetrically using a Lachat AE Flow Injection Auto Analyzer (Method 12-115-01-1-Q, Lachat Instruments, Inc., Milwaukee, WI, USA).

Phospholipid Fatty Acid Analysis

We used phospholipid fatty acids (PLFAs) to determine differences in the microbial biomass (MB) and the ratios of fungal to bacterial biomass. Briefly, total lipids were extracted using 10 ml of methanol, 5 ml chloroform, and 4 ml of a 50 mM phosphate buffer (pH = 7.4) from 5 g of lyophilized soil (White *et al.* 1979; DeForest *et al.*2004). To determine analytical recovery, phospholipid 19:0 (1,2-dinonadecanoyl-*sn* -glycero-3-phosphocholine) and 21:0 (1,2-diheneicosanoyl-*sn* -glycero-3-phosphocholine) standards (Avanti Polar Lipids, Inc., Alabaster, AL, USA) were added during the extraction phase (DeForest *et al.* 2012). Polar lipids were separated from other lipids using silicic acid solid-phase chromatography columns (500 mg 6 ml^{-1}; Thermo Scientific, Waltham, MA, USA), and the separated polar lipids were converted to fatty acid methyl esters (FAME) through methanolysis (Guckert *et al.* 1985). The resulting FAMEs were separated using a HP GC-FID (HP6890 series, Agilent Technologies, Inc. Santa Clara, CA, USA) gas chromatograph, and peaks/biomarkers were identified using the Sherlock System (v. 6.1, MIDI, Inc., Newark, DE, USA). External FAME standards (K104 FAME mix, Grace, Deerfield, IL, USA) were used to determine concentrations. The sum of all detected 14–19 C-length PLFAs was used to calculate MB because longer PLFAs can be indicators of mosses and higher plants (Zelles 1999). Ratios of fungal to bacterial biomass (fungi:bacteria) were calculated by dividing the amount (mol) of the fungal biomarker 18:2ω6c by the sum of all other microbial biomarkers (i.e., mol 18:2ω6c /(mol MB – mol 18:2ω6c)).

Extracellular enzyme activity

We measured potential extracellular enzyme activity of α-glucosidase (AG), β-glucosidase (BG), cellobiohydrolase (CB), β-xylosidase (BX), N-acetylglucosaminidase (NAG), leucine aminopeptidase (LAP), and acid phosphatase (AP) fluorometrically following Bell *et al.* (2013). Briefly, an 800 µl soil slurry consisting of 2.75 g of field-moist soil in 91 ml of 50 mM sodium acetate buffer (pH = 5.5) was incubated with 200 µl of each of the 100 µM 4-methylumbelliferone (MUB)-linked or 7-amido-4-methylcoumarin (AMC)-linked substrates (only LAP was AMC-linked) in 96-deep well plates. After a 3-h incubation at 20 °C, plates were centrifuged, and the supernatant was transferred to black, flat-bottom 96-well plates. Fluorescence was measured on a Tecan M200 Pro (Tecan Group Ltd., Männedorf, Switzerland) using an excitation wavelength of 365 nm and an emission wavelength of 450 nm.

The enzymes, AG, BG, BX, and CB are involved in the degradation of organic C, and total C-acquiring enzyme activity (C_{sum}) was operationally defined as the sum of these four enzyme activities. The enzyme, NAG is involved in releasing N-acetylglucosamine from aminopolysaccharides such as chitin and peptidoglycan, and LAP catalyzes the hydrolysis of leucine residues at the N-terminus of peptides and proteins. Both NAG and LAP are considered N-acquiring enzymes and were similarly summed to define the variable N_{sum}, which we use as a proxy for N acquisition by decomposition. Acid phosphatase is involved in releasing phosphate from monoester bonds, representing a P-mineralizing enzyme (Burns *et al.* 2013).

Extracellular enzyme activities were expressed per soil mass (mmol EE activity kg^{-1} soil h^{-1}), SOC (mmol EE activity kg^{-1} SOC h^{-1}), and MB (mmol EE activity kg^{-1} MB h^{-1}). These latter two variables are called SOC-normalized and MB-normalized, respectively in this paper. We also measured the ratio of C-, N-, and

P-acquiring enzymes. Because EEs mediate nutrient acquisition for soil microorganisms, they can be used to determine relative nutrient demand (Olander & Vitousek 2000; Sinsabaugh & Shah 2012). Hence, we used C_{sum}:N_{sum}, C_{sum}:AP, and N_{sum}:AP as proxies for C:N, C:P, and N:P relative demand ratios, respectively.

Statistical analysis

All statistical tests and visualizations were conducted in R (R Development Core Team 2008) using the lme4 (Bates *et al.* 2015) and MuMin (Barton 2018) packages. We used mixed-effects models with site as a random effect to examine the relationship between depth, SOC, MB, clay, and fungi:bacteria and EE activity (expressed on soil mass, SOC, and MB bases). We similarly used mixed-effects models with site as a random effect to examine the effect of soil stoichiometry (using ratios of SOC, total N, and available P) on enzyme stoichiometry. These models were conducted on the complete dataset, the surface soil dataset (depth < 20 cm), and the subsoil dataset (depth > 20 cm) to determine differences in the controls of EE activities between the surface and subsoils. Because we did not characterize the horizonation of the sampling pits, we *a priori* chose 20 cm to represent the subsoil because most EE studies do not sample below this depth. However, we also conducted our analysis using a 30 cm threshold, and statistical significance and overall interpretation remained unchanged. Therefore, for clarity, we report results using only the 20 cm threshold for the subsoil. To report the variance explained by the model, we report the marginal R^2 value, which expresses the increase in explained variance by including the fixed effect(s) (Nakagawa & Schielzeth 2013). We also used analysis of variance (ANOVA) to determine if the fraction of EE activity below 20 cm differed by soil order. We assessed significance at the $\alpha = 0.05$ level and marginal significance at $\alpha = 0.10$. If significant differences were detected, we used Tukey's Test of Honest Significant Differences to determine which soil orders were significantly different.

We used QQ-plots and scale-location plots to inspect normality and homoscedasticity, respectively. Because many of the mixed-effects models failed to meet parametric assumptions, all dependent and independent continuous variables were natural log-transformed and re-analyzed. The resulting models, along with the ANOVAs, met the assumptions of parametric tests. For visualization purposes, data are left untransformed unless otherwise stated.

RESULTS

Whole profile soil properties among sites

Soil organic C, total N, available P, and fungi:bacteria decreased while clay percentage increased with depth across the CZO network (all: $p < 0.001$, Fig. S1A-E). Across all sites, soil pH was relatively constant throughout the depth profile ($p = 0.236$, Fig. S1F). However, some individual sites showed decreases (e.g., SCST: $p = 0.036$) or increases (e.g., HARD: $p = 0.040$, PROV: $p = 0.003$) in pH with depth.

Distribution of extracellular enzyme activity is related to microbial biomass and organic carbon throughout the top meter of soil

For all assayed EEs, EE activity per mass of soil declined logarithmically with depth ($p < 0.001$, Fig. 1 and S2), but about 50% of the total-profile EE activity kg^{-1} soil in the top meter occurred below 20 cm (Fig. 2A). However, the proportion of the EE activity below 20 cm differed by the soil order for many of the assayed EEs (Table S1). Mollisols had about a 1.5 times greater percentage of the sum of C- and N-acquiring EE activity kg^{-1} soil below 20 cm than Inceptisols or Ultisols ($p < 0.050$ for all comparisons, Fig. 2B). For AP, the 39% higher proportion in the subsoil for Mollisols compared to Inceptisols was only marginally significant ($p = 0.063$).

There were also differences in the percentage of MB and SOC in the subsoil among soil orders (MB: $p < 0.001$, SOC: $p = 0.013$), with Mollisols having an almost two times greater proportion of MB and SOC below 20 cm than Inceptisols (MB: $p = 0.006$, SOC: $p = 0.013$; Fig. 2B). While the proportion of MB below 20 cm was significantly higher in Mollisols compared to Ultisols (about 1.5 times greater, $p = 0.001$), the difference in the proportion of SOC below 20 cm between Mollisols and Ultisols was only marginally significant ($p = 0.057$).

Microbial biomass-normalized EE activity increased with depth for all enzymes (Fig. S3; all: $p < 0.05$). The strongest increases were for LAP and AP, which increased six- and seven-fold, respectively, while NAG and BG increased by 85% and 103%, respectively. Throughout the top meter, over 80% of MB-normalized EE activity occurred below 20 cm (Fig. S4A). However, because the proportion of MB below 20 cm also varied among soil orders, the proportion of MB-normalized EE activity below 20 cm was consistent among soil orders for most assayed EEs (AG: $p = 0.333$, BG: $p = 0.175$, CB: $p = 0.278$, BX: $p = 0.211$, NAG: $p = 0.027$, LAP: $p = 0.537$, AP: $p = 0.048$; Fig. S4A). Nevertheless, the proportion of MB-normalized NAG activity below 20 cm was 15% greater in Ultisols compared to Inceptisols ($p = 0.025$), and the proportion of MB-normalized AP activity below 20 cm was 17% greater in Ultisols compared to Mollisols ($p = 0.042$).

There were inconsistent patterns of EE activity normalized by SOC with depth. N-acetylglucosaminidase normalized by SOC decreased with depth ($p = 0.004$); AG, LAP, and AP increased with depth (AG: $p = 0.016$, LAP: $p = 0.002$, AP: $p < 0.001$), and BG, CB, and BX did not change with depth (BG: $p = 0.322$, CB: $p = 0.344$, BX: $p = 0.198$; Fig. S5). Similar to the proportion of MB-normalized EE activity below 20 cm, the proportion of EE normalized by SOC below 20 cm averaged about 80% and did not differ among soil orders (all: $p > 0.1$; Fig. S6).

Controls on extracellular enzyme activity throughout the top meter of soil

Consistently, MB, SOC, and fungi:bacteria were better predictors of EE activities per mass of soil than pH or clay concentrations (Table S2). This was generally consistent among surface soil- and subsoil-only datasets except for fungi:bacteria, which was only a strong predictor in the surface soil (Table S3).

Normalized by SOC or MB, soil pH was generally not a significant predictor of the assayed EE activities. The exception was LAP kg^{-1} SOC, which correlated positively with pH ($p = 0.037$; all other EEs: $p > 0.05$; Table S4), a pattern that was consistent among surface soil- and subsoil-only datasets (Table 2). In contrast, when EE activities were normalized per unit MB, clay concentrations and fungi:bacteria were generally correlated positively with EE activities (Table S4). When surface and subsoil EE data were analyzed separately, the effect of clay concentrations and fungi:bacteria on MB-normalized EE activities was more often significant in the subsoil (Table 2).

Relating soil and extracellular enzyme stoichiometries throughout the top meter of soil

When considering soils from all depth increments, only $soil_{C:N}$ and $EE_{C:N}$ were correlated (C:N: $p = 0.013$, C:P: $p = 0.292$, N:P: $p = 0.276$), but this negative correlation between $soil_{C:N}$ and $EE_{C:N}$was relatively weak (marginal $R^2 = 0.038$; Fig. S7). However, using the surface soil-only dataset, all soil and EE stoichiometries were negatively correlated (C:N: $p = 0.003$, marginal $R^2 = 0.268$; C:P: $p = 0.002$, marginal $R^2 = 0.193$; N:P: $p = 0.004$, marginal $R^2 = 0.260$; Figure 3). In the subsoil, these correlations decoupled such that none of the stoichiometries were significantly correlated (C:N: $p = 0.288$, C:P: $p = 0.358$, N:P: $p = 0.282$; Fig. 3).

DISCUSSION

Our continental-scale sampling efforts show that microbial activity at depth is non-negligible, and the relative proportion of EE activity (g^{-1} soil) at depth depends predominately on soil development (i.e., soil order; Fig. 2B). This is likely due to changes in the vertical distribution of substrate (organic C) and MB among these soil orders (Batjes 1996; Fig. 2B), which strongly correlate with EE activity (Sinsabaugh *et al.* 2008; Table S2). Hence, we show that SOC and MB are the strongest controls of EE activities throughout the soil profile.

Increases in the MB-normalized EE activities at depth suggest an accumulation of stabilized EEs. While MB-normalized EE activity is often related to the relative activity of the microbial community or differences in metabolic strategies among microbial taxa (Boerner*et al.* 2005), we alternatively hypothesize that the increase in MB-normalized EE activity is due to EE stabilization, namely the sorption of the EEs onto clay or organic matter particles that impedes EE degradation (Sarkar *et al.* 1989, Burns *et al.* 2013). Because EE activities are often measured in a salt-buffered soil slurry that disrupts the stabilization of EEs (as is the case in our study), EE activity assays generally measure both active and stabilized EEs (Burns*et al.* 2013). We hypothesize that higher subsoil MB-normalized EE activities with depth is primarily a product of EE

stabilization instead of differences in the metabolic qualities of the microbial community for three reasons. First of all, MB-normalized respiration (i.e., microbial metabolic quotient), which is another measure of the relative activity of the microbial community, generally does not increase with depth (Dominy & Haynes 2002; Fang & Moncrieff 2005; but see Lavahun *et al.* 1996). Secondly, the relative abundance of fungi, which produce more EEs per unit MB than bacteria (Romaní *et al.* 2006), decreased with depth. Finally, the decoupling of soil stoichiometry and EE stoichiometry at depth suggests that EE activities are not responsive to altered nutrient availabilities. Taken together, these results suggest that the physiochemical process of EE stabilization, a largely abiotic process, is the major control of EE activity in the subsoil.

Extracellular enzyme stabilization as a major mechanism in the subsoil is corroborated by our finding that the influence of clay concentration on MB-normalized EE activity is higher in the subsoil than the surface soil (Table 2). Furthermore, we may have underestimated EE activity in high clay soils because clay can increase the pH optima of EEs 1-2 pH units (McLaren & Estermann 1957; Ramírez-Martínez & McLaren 1966). Whereas many EEs have native pH optima between 4-6.5 (Parham & Deng 2000; Niemi & Vepsäläinen 2005; Turner 2010; Min *et al.* 2014), an increase of two pH units would be significantly higher than the pH of our assay buffer (pH = 5.5). Therefore, we conclude that EE stabilization is a major process when microbial activity is relatively low and clay concentrations are relatively high, which is often the case in subsurface soil layers.

Extracellular enzyme stabilization could be partially responsible for the muted treatment effects on subsoil EE activity commonly found throughout the literature (e.g., Kramer *et al.* 2013; Jing*et al.* 2017; Yao *et al.* 2019). When the stabilized EE pool is significantly greater than the active EE pool, the ability to detect changes in the active pool is decreased. For example, if we assume that there is negligible EE stabilization in the surface soil and that the actualized MB-normalized EE activity *in situ* is constant throughout the soil profile, our results show that across our study sites at least 29-71% of the assayed MB-normalized EE activity at depth can be attributed to stabilized EEs, depending on the EE (Equation 1).

$Z = ((Y - X)/Y) * 100$

X = Average MB-normalized EE activity in surface soil

Y = Average MB-normalized EE activity in subsoil

Z = Percent MB-normalized EE activity in subsoil attributed to stabilized EEs

This calculation likely represents the lower bound of the estimated stabilized MB-normalized EE activity because any stabilization in the surface soil (X), would increase Z, and the relative proportion of fungal biomass, which release comparatively more EEs than bacteria per unit MB (Romaní *et al.* 2006), decreased with depth. Nevertheless, this implies that if the stabilized EE pool is resistant to treatment effects in experiments (e.g., Kramer *et al.* 2013; Jing *et al.* 2017; Yao *et al.* 2019), the ability to detect significant changes in microbial activity at depth using EE assays at depth is also reduced by at least 29-71%. In instances where the magnitude of the treatment effect is modest, it is unlikely that a significant change in subsoil EE activity will be detected. However, this should not necessarily be interpreted as a lack of microbial response, and caution should be exercised in interpreting the effect of a surface manipulation or treatment on subsoil EE activity.

The discrepancy between soil and EE stoichiometry at depth may also be caused by the increased discontinuity of substrates in the subsoil and the reduced ability of the microbial community to respond to changes in resource availability (Allison *et al.* 2007). This would prevent subsoil microorganisms altering their EE stoichiometry to different nutrient conditions. Resource availability is typically higher in surface soils than in subsoils (Salomé *et al.* 2010). Recent work in soil enzymography show that C-degrading EE activities are enriched only 0.5-2 mm from C-rich rhizodeposits (Ma *et al.* 2018). The EE assays that we and most others employed disrupt the spatial arrangement of EEs and substrates such that our results express bulk EE activities and bulk resource concentrations, which may not be representative of smaller, more localized heterogeneity in resources.

In contrast to earlier work (Sinsabaugh *et al.* 2008), we generally did not find pH to be well-correlated with EE activity (on a soil mass-, MB- , or SOC-basis) at any depth (Table 2, S2-S4). We attribute this discrepancy to differences in methodologies that measure different aspects of the EE pool. Fluorometric measurements in the commonly used microplate EE activity assay are impacted by slurry pH (Burns *et al.* 2013). Therefore, slurries are generally buffered either by a consistent pH (as in our case) or by a pH characteristic of the native soil (as in Sinsabaugh et al. 2008). When buffered by a constant pH (near pH optima), EE activities better reflect the size of the EE pool, whereas EE activity assays buffered by a pH corresponding to the native soil better reflect *in situ* rates of EE activity (Burns *et al.* 2013). Sinsabaugh et al. (2008) buffered soil slurries from alkaline soils at pH 8 and found that BG, CB, NAG, and AP activity kg^{-1} SOC decreased with soil pH, while LAP kg^{-1} C increased. However, across multiple biomes, BG, CB, and NAG have acidic pH optima (4-6.5; Parham & Deng 2000; Niemi & Vepsäläinen 2005; Turner 2010; Min *et al.* 2014). Thus, the decrease in BG, CB, and NAG activity kg^{-1} C with greater soil pH in Sinsabaugh *et al.* (2008) could be caused by a buffer pH for alkaline soils that is higher than the pH optima of the EEs. Because this buffer pH was chosen to reflect *in situ*conditions (Burns *et al.* 2013), we conclude that across ecosystems, *in situ* rates of BG, CB, and NAG activity are likely lower in alkaline soils because of discrepancies between EE pH optima and *in situ* soil pH. Soil pH can affect EE concentrations through its impact on the microbial communities (e.g., Acosta-Martínez & Tabatabai 2000; Ekenler & Tabatabai 2003; Stark *et al.* 2014); however, we find little evidence for an effect of soil pH on the size of the EE pool across the wide range of soil types studied here.

Taken together, our results suggest that the relative importance of the different controls on EE activities change with depth. We summarize this in a conceptual model, where the active EE pool is controlled by microbial EE production (proximately influenced by MB and resource demand), and the stabilized EE pool is primarily influenced by EE stabilization onto clay particles (Figure 4). Because MB and resource demand decrease with depth as C becomes more limiting and clay concentrations increase, the subsoil total EE pool is maintained because of the relatively large proportion of stabilized (sorbed on soil colloids) EEs that decay slower than unstabilized (present in the bulk soil solution) EEs. Understanding how soil texture affects EE stabilization and decay dynamics is a critical knowledge gap in enzyme-explicit microbial models (e.g., Schimel & Weintraub 2003; Manzoni *et al.* 2016; Abramoff *et al.* 2017; Sulman *et al.* 2018). For instance, Schimel *et al.* (2017) estimated EE decay dynamics in multiple soils by measuring EE activities for weeks after sterilization. While these soils varied in texture, there did not appear to be a consistent pattern between soil texture and EE decay, possibly because of changes in other edaphic factors (i.e., moisture, substrate, etc.). Future work should systematically study EE decay and its relation to multiple edaphic factors including clay concentration to test our proposed conceptual model.

Overall, our results imply that the vast majority of EE studies are missing a large portion of the total EE activity in soils, and that the unmeasured subsoil EE activity varies in its response to environmental conditions. Therefore, one cannot simply extrapolate surface soil EE values into the subsoil. As numerous other experiments have shown (Blume*et al.* 2002; Taş *et al.* 2014; Hicks Pries *et al.*2017), ignoring subsoils and exclusively focusing on surface soils can limit our ability to understand whole-profile EE-dynamics and soil C storage.

ACKNOWLEDGEMENTS

We thank N. Blair, A. Bissett, T. Brewer, A.N. Campbell, G. King, M. Firestone, M. Leon, G. Logan, N. Lu, F. Meyer, S.M. Owens, A. Packman, A.F. Plante, D.D. Richter, W.L. Silver and E. Starr for their contributions to this research effort and B. Boudinot for assistance with PLFA analysis. This research was supported by the NSF EarthCube program (ICER-1541047), the Critical Zone Observatory Network (EAR-1331939), and a University of California Merced Graduate Fellowship Award derived from a match provided by the Southern Sierra Critical Zone Observatory (to NCD). Work conducted by researchers at Lawrence Livermore National Laboratory was performed under the auspices of the U.S. Department of Energy by under contract DE-AC52-07NA27344, and supported by a US Department of Energy Early Career Research Program Award to J. Pett-Ridge (SCW1478). Support for this research was also provided by National Science Foundation for RC CZO Cooperative agreement, EAR-1331872.

LITERATURE CITED

Abramoff, R.Z., Davidson, E.A. & Finzi, A.C. (2017). A parsimonious modular approach to building a mechanistic belowground carbon and nitrogen model. *J. Geophys. Res. Biogeosci.* , 122, 2017JG003796.

Acosta-Martínez, V. & Tabatabai, M.A. (2000). Enzyme activities in a limed agricultural soil. *Biol Fertil Soils* , 31, 85–91.

Allison, S.D., Gartner, T.B., Holland, K., Weintraub, M. & Sinsabaugh, R.L. (2007). Soil Enzymes: Linking Proteomics and Ecological Processes.*Manual of Environmental Microbiology, Third Edition* , 704–711.

Barton, K. (2018). *MuMIn: Multi-Model Inference* .

Bates, D., Maechler, M., Bolker, B. & Walker, S. (2015). Fitting Linear Mixed-Effects Models Using lme4. *Journal of Statistical Software* , 67, 1–48.

Batjes, N. H. (1996). Total carbon and nitrogen in the soils of the world. *European Journal of Soil Science* , 47, 151–163.

Bell, C.W., Fricks, B.E., Rocca, J.D., Steinweg, J.M., McMahon, S.K. & Wallenstein, M.D. (2013). High-throughput Fluorometric Measurement of Potential Soil Extracellular Enzyme Activities. *Journal of Visualized Experiments* .

Billings, S.A. & Ballantyne, F. (2013). How interactions between microbial resource demands, soil organic matter stoichiometry, and substrate reactivity determine the direction and magnitude of soil respiratory responses to warming. *Global Change Biology* , 19, 90–102.

Birge, H.E., Conant, R.T., Follett, R.F., Haddix, M.L., Morris, S.J., Snapp, S.S., *et al.* (2015). Soil respiration is not limited by reductions in microbial biomass during long-term soil incubations.*Soil Biology and Biochemistry* , 81, 304–310.

Blume, E., Bischoff, M., Reichert, J.M., Moorman, T., Konopka, A. & Turco, R.F. (2002). Surface and subsurface microbial biomass, community structure and metabolic activity as a function of soil depth and season.*Applied Soil Ecology* , 20, 171–181.

Boerner, R.E.J., Brinkman, J.A. & Smith, A. (2005). Seasonal variations in enzyme activity and organic carbon in soil of a burned and unburned hardwood forest. *Soil Biology and Biochemistry* , 37, 1419–1426.

Brewer, T.E., Aronson, E.L., Arogyaswamy, K., Billings, S.A., Botthoff, J.K., Campbell, A.N., *et al.* (2019). Ecological and Genomic Attributes of Novel Bacterial Taxa That Thrive in Subsurface Soil Horizons. *mBio* , 10, e01318-19.

Brubaker, S.C., Jones, A.J., Lewis, D.T. & Frank, K. (1993). Soil Properties Associated with Landscape Position. *Soil Science Society of America Journal* , 57, 235–239.

Burns, R.G., DeForest, J.L., Marxsen, J., Sinsabaugh, R.L., Stromberger, M.E., Wallenstein, M.D., *et al.* (2013). Soil enzymes in a changing environment: Current knowledge and future directions.*Soil Biology and Biochemistry* , 58, 216–234.

Chen, H., Li, D., Zhao, J., Xiao, K. & Wang, K. (2018). Effects of nitrogen addition on activities of soil nitrogen acquisition enzymes:A meta-analysis. *Agriculture, Ecosystems & Environment* , 252, 126–131.

DeForest, J.L., Smemo, K.A., Burke, D.J., Elliott, H.L. & Becker, J.C. (2012). Soil microbial responses to elevated phosphorus and pH in acidic temperate deciduous forests. *Biogeochemistry* , 109, 189–202.

DeForest, J.L., Zak, D.R., Pregitzer, K.S. & Burton, A.J. (2004). Atmospheric nitrate deposition and the microbial degradation of cellobiose and vanillin in a northern hardwood forest. *Soil Biology and Biochemistry* , 36, 965–971.

Dick, R.P., Dick, L.K., Deng, S., Li, X., Kandeler, E., Poll, C.,*et al.* (2018). Cross-laboratory comparison of fluorimetric microplate and colorimetric bench-scale soil enzyme assays. *Soil Biology and Biochemistry* , 121, 240–248.

Dominy, C. & Haynes, R. (2002). Influence of agricultural land management on organic matter content, microbial activity and aggregate stability in the profiles of two Oxisols. *Biol Fertil Soils* , 36, 298–305.

Dove, N.C., Stark, J.M., Newman, G.S. & Hart, S.C. (2019). Carbon control on terrestrial ecosystem function across contrasting site productivities: the carbon connection revisited. *Ecology* , 100, e02695.

Eilers, K.G., Debenport, S., Anderson, S. & Fierer, N. (2012). Digging deeper to find unique microbial communities: The strong effect of depth on the structure of bacterial and archaeal communities in soil.*Soil Biology and Biochemistry* , 50, 58–65.

Ekenler, M. & Tabatabai, M.A. (2003). Effects of liming and tillage systems on microbial biomass and glycosidases in soils. *Biol Fertil Soils* , 39, 51–61.

Fang, C. & Moncrieff, J.B. (2005). The variation of soil microbial respiration with depth in relation to soil carbon composition.*Plant Soil* , 268, 243–253.

Gee, G.W. & Bauder, J.W. (2018). Particle-size Analysis. In:*Methods of Soil Analysis* . John Wiley & Sons, Ltd, pp. 383–411.

Guckert, J.B., Antworth, C.P., Nichols, P.D. & White, D.C. (1985). Phospholipid, ester-linked fatty acid profiles as reproducible assays for changes in prokaryotic community structure of estuarine sediments.*FEMS Microbiol Ecol* , 1, 147–158.

Hicks Pries, C.E., Castanha, C., Porras, R.C. & Torn, M.S. (2017). The whole-soil carbon flux in response to warming. *Science* , 355, 1420–1423.

Jing, X., Chen, X., Tang, M., Ding, Z., Jiang, L., Li, P., *et al.*(2017). Nitrogen deposition has minor effect on soil extracellular enzyme activities in six Chinese forests. *Science of The Total Environment* , 607–608, 806–815.

Jobbagy, E.G. & Jackson, R.B. (2000). The vertical distribution of soil organic carbon and its relation to climate and vegetation.*Ecological Applications* , 10, 423–436.

Jones, D.L., Magthab, E.A., Gleeson, D.B., Hill, P.W., Sanchez-Rodriguez, A.R., Roberts, P., *et al.* (2018). Microbial competition for nitrogen and carbon is as intense in the subsoil as in the topsoil. *Soil Biology and Biochemistry* , 117, 72–82.

Kivlin, S.N. & Treseder, K.K. (2014). Soil extracellular enzyme activities correspond with abiotic factors more than fungal community composition. *Biogeochemistry* , 117, 23–37.

Kramer, S., Marhan, S., Haslwimmer, H., Ruess, L. & Kandeler, E. (2013). Temporal variation in surface and subsoil abundance and function of the soil microbial community in an arable soil. *Soil Biology and Biochemistry* , 61, 76–85.

Lavahun, M.F.E., Joergensen, R.G. & Meyer, B. (1996). Activity and biomass of soil microorganisms at different depths. *Biol Fertil Soils* , 23, 38–42.

Loeppmann, S., Blagodatskaya, E., Pausch, J. & Kuzyakov, Y. (2016). Enzyme properties down the soil profile - A matter of substrate quality in rhizosphere and detritusphere. *Soil Biology and Biochemistry* , 103, 274–283.

Ma, X., Zarebanadkouki, M., Kuzyakov, Y., Blagodatskaya, E., Pausch, J. & Razavi, B.S. (2018). Spatial patterns of enzyme activities in the rhizosphere: Effects of root hairs and root radius. *Soil Biology and Biochemistry* , 118, 69–78.

Manzoni, S., Moyano, F., Katterer, T. & Schimel, J. (2016). Modeling coupled enzymatic and solute transport controls on decomposition in drying soils. *Soil Biology and Biochemistry* , 95, 275–287.

McLaren, A.D. & Estermann, E.F. (1957). Influence of pH on the activity of chymotrypsin at a solid-liquid interface. *Archives of Biochemistry and Biophysics* , 68, 157–160.

Min, K., Lehmeier, C.A., Ballantyne, F., Tatarko, A. & Billings, S.A. (2014). Differential effects of pH on temperature sensitivity of organic carbon and nitrogen decay. *Soil Biology and Biochemistry* , 76, 193–200.

Nakagawa, S. & Schielzeth, H. (2013). A general and simple method for obtaining R2 from generalized linear mixed-effects models. *Methods in Ecology and Evolution* , 4, 133–142.

Nannipieri, P., Trasar-Cepeda, C. & Dick, R.P. (2018). Soil enzyme activity: a brief history and biochemistry as a basis for appropriate interpretations and meta-analysis. *Biol Fertil Soils* , 54, 11–19.

Niemi, R.M. & Vepsalainen, M. (2005). Stability of the fluorogenic enzyme substrates and pH optima of enzyme activities in different Finnish soils. *J. Microbiol. Methods* , 60, 195–205.

Olander, L.P. & Vitousek, P.M. (2000). Regulation of Soil Phosphatase and Chitinase Activity by N and P Availability. *Biogeochemistry* , 49, 175–190.

Olsen, S.R., Cole, C.V., Watanabe, F.S. & Dean, L.A. (1954).*Estimation of available phosphorus in soils by extraction with sodium bicarbonate* (USDA Circular No. 939). U.S. Government Printing Office, Washington, D.C., USA.

Parham, J.A. & Deng, S.P. (2000). Detection, quantification and characterization of β-glucosaminidase activity in soil. *Soil Biology and Biochemistry* , 32, 1183–1190.

Paul, E.A., Follett, R.F., Leavitt, S.W., Halvorson, A., Peterson, G.A. & Lyon, D.J. (1997). Radiocarbon Dating for Determination of Soil Organic Matter Pool Sizes and Dynamics. *Soil Science Society of America Journal* , 61, 1058–1067.

R Development Core Team. (2008). *R: A language and environment for statistical computing* . R Foundation for Statistical Computing, Vienna, Australia.

Ramírez-Martínez, J.R. & McLaren, A.D. (1966). Some factors influencing the determination of phosphatase activity in native soils and in soils sterilized by irradiation. *Enzymologia* , 31, 23–38.

Robertson, P. of C. and S.S.G.P., Robertson, G.P., Coleman, D.C., Sollins, P., Bledsoe, C.S., Bledsoe, P. of S.E. in the D. of L.A. and W.R.C.S., *et al.* (1999). *Standard Soil Methods for Long-term Ecological Research* . Oxford University Press.

Romaní, A.M., Fischer, H., Mille-Lindblom, C. & Tranvik, L.J. (2006). Interactions of Bacteria and Fungi on Decomposing Litter: Differential Extracellular Enzyme Activities. *Ecology* , 87, 2559–2569.

Rumpel, C. & Kögel-Knabner, I. (2010). Deep soil organic matter—a key but poorly understood component of terrestrial C cycle. *Plant Soil* , 338, 143–158.

Rumpel, C., Kögel-Knabner, I. & Bruhn, F. (2002). Vertical distribution, age, and chemical composition of organic carbon in two forest soils of different pedogenesis. *Organic Geochemistry* , 33, 1131–1142.

Salomé, C., Nunan, N., Pouteau, V., Lerch, T.Z. & Chenu, C. (2010). Carbon dynamics in topsoil and in subsoil may be controlled by different regulatory mechanisms. *Global Change Biology* , 16, 416–426.

Sarkar, J.M., Leonowicz, A. & Bollag, J.-M. (1989). Immobilization of enzymes on clays and soils. *Soil Biology and Biochemistry* , 21, 223–230.

Schimel, J., Becerra, C.A. & Blankinship, J. (2017). Estimating decay dynamics for enzyme activities in soils from different ecosystems.*Soil Biology and Biochemistry* , 114, 5–11.

Schimel, J.P. & Weintraub, M.N. (2003). The implications of exoenzyme activity on microbial carbon and nitrogen limitation in soil: a theoretical model. *Soil Biology and Biochemistry* , 35, 549–563.

Schimel, J.P., Wetterstedt, J.Å.M., Holden, P.A. & Trumbore, S.E. (2011). Drying/rewetting cycles mobilize old C from deep soils from a California annual grassland. *Soil Biology and Biochemistry* , 43, 1101–1103.

Schnecker, J., Wild, B., Takriti, M., Eloy Alves, R.J., Gentsch, N., Gittel, A., *et al.* (2015). Microbial community composition shapes enzyme patterns in topsoil and subsoil horizons along a latitudinal transect in Western Siberia. *Soil Biology and Biochemistry* , 83, 106–115.

Sinsabaugh, R.L., Hill, B.H. & Follstad Shah, J.J. (2009). Ecoenzymatic stoichiometry of microbial organic nutrient acquisition in soil and sediment. *Nature* , 462, 795–798.

Sinsabaugh, R.L., Lauber, C.L., Weintraub, M.N., Ahmed, B., Allison, S.D., Crenshaw, C., *et al.* (2008). Stoichiometry of soil enzyme activity at global scale. *Ecology Letters* , 11, 1252–1264.

Sinsabaugh, R.L., Manzoni, S., Moorhead, D.L. & Richter, A. (2013). Carbon use efficiency of microbial communities: stoichiometry, methodology and modelling. *Ecol Lett* , 16, 930–939.

Sinsabaugh, R.L. & Shah, J.J.F. (2011). Ecoenzymatic stoichiometry of recalcitrant organic matter decomposition: the growth rate hypothesis in reverse. *Biogeochemistry* , 102, 31–43.

Sinsabaugh, R.L. & Shah, J.J.F. (2012). Ecoenzymatic Stoichiometry and Ecological Theory. *Annual Review of Ecology, Evolution, and Systematics* , 43, 313–343.

Stark, S., Männistö, M.K. & Eskelinen, A. (2014). Nutrient availability and pH jointly constrain microbial extracellular enzyme activities in nutrient-poor tundra soils. *Plant Soil* , 383, 373–385.

Stone, M.M., DeForest, J.L. & Plante, A.F. (2014). Changes in extracellular enzyme activity and microbial community structure with soil depth at the Luquillo Critical Zone Observatory. *Soil Biology and Biochemistry* , 75, 237–247.

Sulman, B.N., Moore, J.A.M., Abramoff, R., Averill, C., Kivlin, S., Georgiou, K., *et al.* (2018). Multiple models and experiments underscore large uncertainty in soil carbon dynamics.*Biogeochemistry* , 141, 109–123.

Taş, N., Prestat, E., McFarland, J.W., Wickland, K.P., Knight, R., Berhe, A.A., *et al.* (2014). Impact of fire on active layer and permafrost microbial communities and metagenomes in an upland Alaskan boreal forest. *ISME J* , 8, 1904–1919.

Taylor, J.P., Wilson, B., Mills, M.S. & Burns, R.G. (2002). Comparison of microbial numbers and enzymatic activities in surface soils and subsoils using various techniques. *Soil Biology and Biochemistry* , 34, 387–401.

Trumbore, S.E., Chadwick, O.A. & Amundson, R. (1996). Rapid Exchange Between Soil Carbon and Atmospheric Carbon Dioxide Driven by Temperature Change. *Science* , 272, 393–396.

Turner, B.L. (2010). Variation in pH Optima of Hydrolytic Enzyme Activities in Tropical Rain Forest Soils. *Appl. Environ. Microbiol.* , 76, 6485–6493.

Turner, S., Schippers, A., Meyer-Stüve, S., Guggenberger, G., Gentsch, N., Dohrmann, R., *et al.* (2014). Mineralogical impact on long-term patterns of soil nitrogen and phosphorus enzyme activities.*Soil Biology and Biochemistry* , 68, 31–43.

Waring, B.G., Weintraub, S.R. & Sinsabaugh, R.L. (2014). Ecoenzymatic stoichiometry of microbial nutrient acquisition in tropical soils.*Biogeochemistry* , 117, 101–113.

Weintraub, M.N. & Schimel, J.P. (2003). Interactions between Carbon and Nitrogen Mineralization and Soil Organic Matter Chemistry in Arctic Tundra Soils. *Ecosystems* , 6, 0129–0143.

White, D.C., Davis, W.M., Nickels, J.S., King, J.D. & Bobbie, R.J. (1979). Determination of the sedimentary microbial biomass by extractible lipid phosphate. *Oecologia* , 40, 51–62.

Xiao, W., Chen, X., Jing, X. & Zhu, B. (2018). A meta-analysis of soil extracellular enzyme activities in response to global change. *Soil Biology and Biochemistry* , 123, 21–32.

Yao, Y., Shao, M., Fu, X., Wang, X. & Wei, X. (2019). Effects of shrubs on soil nutrients and enzymatic activities over a 0–100 cm soil profile in the desert-loess transition zone. *CATENA* , 174, 362–370.

Zelles, L. (1999). Fatty acid patterns of phospholipids and lipopolysaccharides in the characterisation of microbial communities in soil: a review. *Biol Fertil Soils* , 29, 111–129.

TABLES

Table 1 : Characteristics of the 19 study sites across ten Critical Zone Observatories (CZOs).

Site	CZO	Latitude	Longitude	$pH_{1:1(water)}$[1]	Elevation (m)	Elevation (m)	Elevation (m)	MAP (
AGRI	Christina	39.8622	-75.7834	4.57 - 7.03	4.57 - 7.03	105	105	1145
BSLT	Reynolds Creek	43.1171	-116.7258	7.69 - 9.40	7.69 - 9.40	1917	1917	479
CTNA	Catalina-Jemez	32.4293	-110.7610	4.62 - 5.87	4.62 - 5.87	2100	2100	840
FLUD	Christina	39.8625	-75.7830	5.86 - 6.33	5.86 - 6.33	113	113	1145
GARN	Shale Hills	40.6949	-77.9199	3.34 - 4.99	3.34 - 4.99	554	554	1050
GOOS	IML	40.4374	-88.5552	7.79 - 8.34	7.79 - 8.34	250	250	1000
GRNT	Reynolds Creek	43.1927	-116.8105	8.91 - 9.29	8.91 - 9.29	1565	1565	616
HARD	Calhoun	34.6064	-81.7234	7.96 - 8.79	7.96 - 8.79	183	183	1250
ICAC	Luquillo	18.2814	-65.7909	4.21 - 4.67	4.21 - 4.67	690	690	5000
LVRD	Luquillo	18.3237	-65.8185	4.23 - 5.64	4.23 - 5.64	343	343	3456
MEAD	Boulder Creek	40.0210	-105.4796	6.56 - 7.75	6.56 - 7.75	2642	2642	519
NSLP	Boulder Creek	40.0125	-105.4690	6.36 - 9.81	6.36 - 9.81	2521	2521	519
PINE	Calhoun	34.6074	-81.7228	–	–	184	184	1250
PRAR	IML	40.4275	-88.6032	7.19 - 7.67	7.19 - 7.67	250	250	1000
PROV	Southern Sierra	37.0675	-119.1950	6.46 - 8.09	6.46 - 8.09	2016	2016	1200
SCST	Catalina-Jemez	32.4263	-110.7612	6.11 - 6.83	6.11 - 6.83	2100	2100	840
SHAL	Shale Hills	40.6640	-77.9064	4.24 - 4.99	4.24 - 4.99	282	282	1050
SJER	Southern Sierra	37.1088	-119.7314	5.90 - 6.25	5.90 - 6.25	405	405	513
MDRN	Eel River	39.7294	-123.6419	–	–	–	487	1500

[1]pH was not measured on PINE and MDRN soils because of limited soil collected.

Table 2 : Marginal R^2 values for mixed-effects models with soil clay concentration, pH, or fungi:bacteria as the sole fixed effect, and soil pit as a random effect on EE activity normalized by microbial biomass (MB) or soil organic carbon (SOC) concentration in top- (< 20 cm) and sub-soils (> 20 cm). Key: α-glucosidase (AG), β-glucosidase (BG), cellobiohydrolase (CB), β-xylosidase (BX), N-acetylglucosamine (NAG), leucine aminopeptidase (LAP), and acid phosphatase (AP) activity. Bolded values represent a significant ($\alpha = 0.05$) effect and +/- signifies the direction of the effect (surface soil: n = 29, subsoil: n = 114).

			MB-normalized[1]	*MB-normalized*[1]	*MB-normalized*[1]	*MB-normalized*[1]	
	Enzyme	Enzyme	Clay	Clay	pH	fungi:bacteria	fungi:ba
Surface soil	*Surface soil*						
	AG	AG	< 0.001	< 0.001	0.020	0.016	0.016
	BG	BG	< 0.001	< 0.001	0.068	0.013	0.013
	CB	CB	0.003	0.003	0.067	0.052	0.052
	BX	BX	0.004	0.004	0.024	0.011	0.011

			MB-normalized[1]	*MB-normalized*[1]	*MB-normalized*[1]	*MB-normalized*[1]	
	NAG	NAG	0.067	0.067	0.009	**+0.298**	**+0.298**
	LAP	LAP	0.004	0.004	0.002	0.007	0.007
	AP	AP	0.004	0.004	0.025	< 0.001	< 0.001
Subsoil	*Subsoil*						
	AG	AG	**+0.097**	**+0.097**	0.006	0.019	0.019
	BG	BG	0.063	0.063	0.025	**+0.171**	**+0.171**
	CB	CB	0.043	0.043	0.034	**+0.037**	**+0.037**
	BX	BX	**+0.094**	**+0.094**	0.002	**+0.146**	**+0.146**
	NAG	NAG	0.020	0.020	0.022	**+0.080**	**+0.080**
	LAP	LAP	0.001	0.001	< 0.001	0.001	0.001
	AP	AP	**+0.142**	**+0.142**	0.025	0.002	0.002

[1] Enzyme activity per unit microbial biomass

[2] Enzyme activity per unit soil organic carbon

FIGURES

Figure 1 : Distribution of activity of α-glucosidase (AG), β-glucosidase (BG), β-xylosidase (BX), cellobiohydrolase (CB), N-acetylglucosaminidase (NAG), leucine aminopeptidase (LAP), and acid phosphatase (AP) per soil mass as a function of depth throughout the top meter of soil across sites. See Table 1 for site abbreviations.

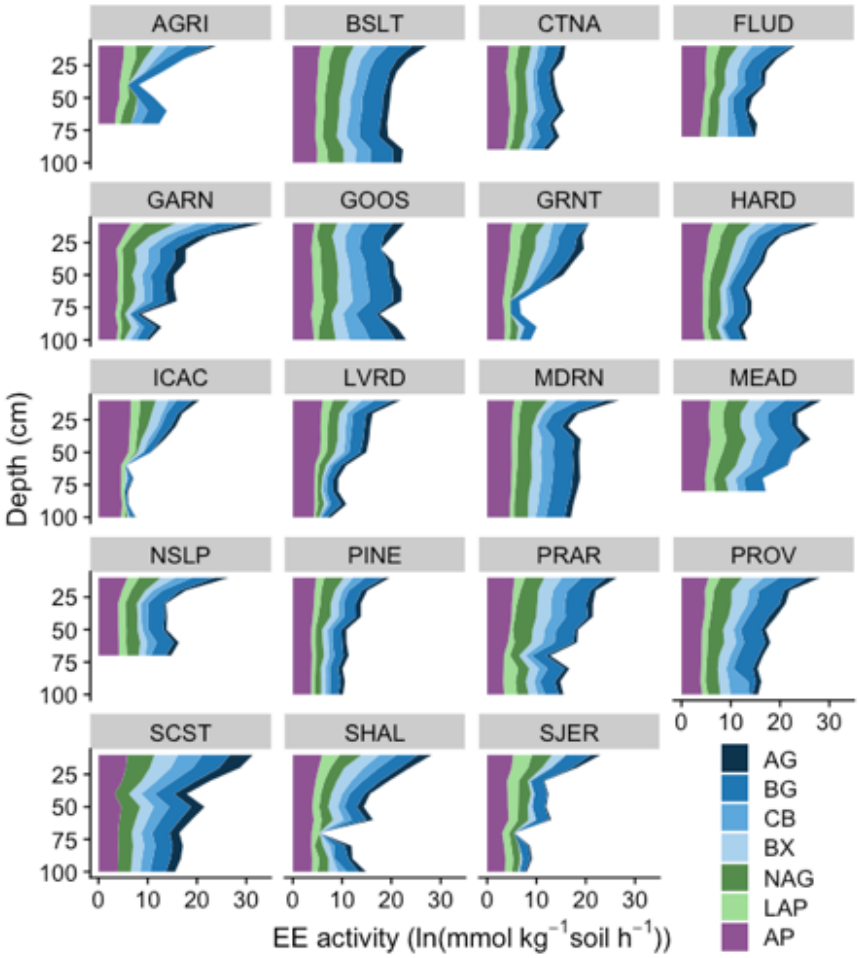

Figure 2 : Percentage of α-glucosidase (AG), β-glucosidase (BG), cellobiohydrolase (CB), β-xylosidase (BX), N-acetylglucosamine (NAG), leucine aminopeptidase (LAP), and acid phosphatase (AP) activity below 20 cm in the top meter (A); and proportion of soil organic carbon (SOC), microbial biomass (MB), sum of C-degrading enzymes (C_{sum}= AG + BG + CB + BX), sum of nitrogen-mineralizing enzymes (N_{sum} = NAG + LAP), and acid phosphatase (AP) below 20 cm in the top meter of soil among soil orders (B). Error bars show ± one standard error of the mean (Figure panel A: n = 19; Figure panel B: Inceptisol: n = 4, Mollisol: n = 5, Ultisol: n = 3).

Figure 3 : Correlations between soil and extracellular enzyme (EE) stoichiometry of carbon (C), nitrogen (N), and phosphorus (P) in surface (< 20 cm depth) and subsoils (> 20 cm depth). Blue lines show significant (α = 0.05) mixed-effects models of the relationship between soil and EE stoichiometry (site was used as a random effect; lines were not drawn where correlations were not significant). Gray ribbons show the standard error of the model. Data points represent individual soil samples (depths within each pit). Note the scales of the axes differ among plots.

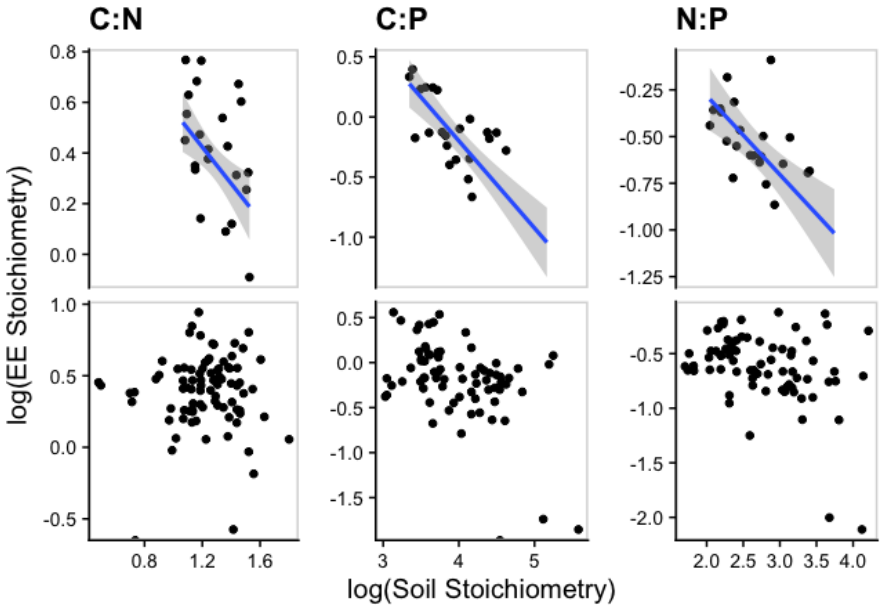

Hosted file

`image4.emf` available at https://authorea.com/users/305676/articles/436472-continental-scale-patterns-of-extracellular-enzyme-activity-in-the-subsoil-an-overlooked-reservoir-of-microbial-activity

Figure 4 : Conceptual model of changing controls on extracellular enzyme activity (EEA) between surface soil and subsoil. Solid lines represent fluxes and dashed lines represent moderating controls. Boxes represent pools or concentrations, and other shapes represent moderating variables. Blue parameters represent microbial parameters, and green boxes represent edaphic variables such as substrate (including carbon [C] and nutrients) and clay concentrations. The differences in the size of boxes between the surface and subsoil represent the relative size of the pool, and differences in the thickness of arrows between the surface and subsoil represent the hypothesized relative magnitude of the flux or control. A portion of the substrate pool is available to microbial biomass (MB) and is moderated by clay concentration and active EEA. Substrate availability moderates substrate demand. Bacterial biomass, fungal biomass, and substrate demand influence active EEA. Additionally, our conceptual model incorporates stabilized EEA (i.e., EEs sorbed onto clay particles), which is primarily influenced by clay concentrations. At depth, the impact of clay on substrate availability and stabilized EEA increases, while the absolute impact of substrates and microbial properties (i.e., microbial biomass and substrate demand) decreases.

SUPPLEMENTAL TABLES

Table S1 : Proportion (and standard error, n = 19) of extracellular enzyme activity (kg^{-1} soil) below 20 cm across the three main soil orders represented in the study. Different superscript letters represent significant differences among soil orders for each enzyme ($\alpha = 0.05$). Key: AG = α-glucosidase, BG = β-glucosidase, CB = cellobiohydrolase, XYL = β-xylosidase, LAP = leucine aminopeptidase, NAG = N-acetylglucosamine, AP = acid phosphatase.

Enzyme	Enzyme	Inceptisols	Mollisols	Ultisols
AG	33.6% (9.6)	33.6% (9.6)	59.5% (8.4)	62.3% (8.3)
BG	40.9% (4.8)^{a}	40.9% (4.8)^{a}	65.1% (5.8)^{b}	46.6% (1.2)^{ab}
CB	41.0% (9.7)	41.0% (9.7)	58.8% (7.6)	36.0% (4.7)
BX	32.2% (4.7)^{a}	32.2% (4.7)^{a}	63.7% (3.1)^{b}	51.8% (6.6)^{b}

Enzyme	Enzyme	Inceptisols	Mollisols	Ultisols
NAG	31.8% (8.1)^{b}	31.8% (8.1)^{b}	65.3% (4.9)^{a}	39.6% (2.8)^{b}
LAP	53.2% (3.1)^{ab}	53.2% (3.1)^{ab}	71.9% (6.8)^{b}	49.0% (5.2)^{a}
AP	47.0% (6.4)	47.0% (6.4)	65.4% (3.7)	56.6% (5.1)

Table S2 : Marginal R^2 values for mixed-effects models with soil microbial biomass (MB), soil organic carbon (SOC) concentration, clay concentration, pH, or fungi:bacteria as the sole fixed effect, and soil pit as a random effect on EE activities (kg^{-1} soil). Key: α-glucosidase (AG), β-glucosidase (BG), cellobiohydrolase (CB), β-xylosidase (BX), N-acetylglucosamine (NAG), leucine aminopeptidase (LAP), acid phosphatase (AP), sum of C-degrading enzymes (C_{sum} = AG + BG + CB + BX), and sum of nitrogen-mineralizing enzymes (N_{sum} = NAG + LAP). Bolded values represent a significant ($\alpha = 0.05$) effect and +/- signifies the direction of the effect (MB, SOC, fungi:bacteria: n = 178, clay and pH: n = 143).

Enzyme	MB (mol PLFA)	SOC (%)	Clay (%)	pH (1:1 w/v H_2O)	fungi:bacteria
C_{sum}	**+0.383**	**+0.341**	**-0.253**	0.002	**+0.046**
AG	**+0.182**	**+0.281**	**-0.120**	0.003	**+0.067**
BG	**+0.433**	**+0.340**	**-0.224**	0.006	**+0.051**
CB	**+0.271**	**+0.293**	**-0.150**	0.006	**+0.043**
BX	**+0.458**	**+0.424**	**-0.231**	0.009	**+0.032**
N_{sum}	**+0.537**	**+0.531**	**-0.280**	0.040	**+0.106**
NAG	**+0.472**	**+0.448**	**-0.239**	0.012	**+0.105**
LAP	**+0.241**	**+0.283**	**-0.246**	0.002	**+0.029**
AP	**+0.497**	**+0.517**	**-0.294**	0.008	**+0.062**

Table S3 : Marginal r^2 values for mixed-effects models with soil microbial biomass (MB), soil organic carbon (SOC) concentration, clay concentration, pH, or fungi:bacteria as the sole fixed effect, and soil pit as a random effect on EE activities (kg^{-1} soil) in surface (< 20 cm) and subsoils (> 20 cm). Key: α-glucosidase (AG), β-glucosidase (BG), cellobiohydrolase (CB), β-xylosidase (BX), N-acetylglucosamine (NAG), leucine aminopeptidase (LAP), acid phosphatase (AP), sum of C-degrading enzymes (C_{sum} = AG + BG + CB + BX), and sum of nitrogen-mineralizing enzymes (N_{sum} = NAG + LAP). Bolded values represent a significant ($\alpha = 0.05$) effect and +/- signifies the direction of the effect (surface soil MB, SOC, fungi:bacteria: n = 38, subsoil MB, SOC, fungi:bacteria: n = 140, surface soil clay & pH: n = 29, subsoil clay and pH: n = 114).

	Enzyme	MB (mol PLFA)	MB (mol PLFA)	MB (mol PLFA)	SOC (%)	Clay (%)	pH (1:1 w/v
Surface soil	*Surface soil*	*Surface soil*					
	C_{sum}	**+0.196**	**+0.196**	**+0.196**	**+0.301**	**-0.200**	0.026
	AG	**+0.186**	**+0.186**	**+0.186**	**+0.320**	0.073	0.002
	BG	**+0.158**	**+0.158**	**+0.158**	**+0.280**	**-0.218**	0.036
	CB	**+0.231**	**+0.231**	**+0.231**	**+0.277**	0.102	0.015
	BX	**+0.197**	**+0.197**	**+0.197**	**+0.240**	**-0.158**	< 0.001
	N_{sum}	**+0.356**	**+0.356**	**+0.356**	**+0.557**	**-0.205**	0.004
	NAG	**+0.367**	**+0.367**	**+0.367**	**+0.555**	**-0.167**	< 0.001
	LAP	**+0.108**	**+0.108**	**+0.108**	**+0.139**	**-0.196**	< 0.001
	AP	**+0.523**	**+0.523**	**+0.523**	**+0.584**	0.126	0.032
Subsoil	*Subsoil*	*Subsoil*					
	C_{sum}	**+0.213**	**+0.213**	**+0.213**	**+0.175**	**-0.090**	0.040
	AG	**+0.041**	**+0.041**	**+0.041**	**+0.069**	0.001	< 0.001
	BG	**+0.285**	**+0.285**	**+0.285**	**+0.185**	**-0.070**	0.042

	Enzyme	MB (mol PLFA)	MB (mol PLFA)	MB (mol PLFA)	SOC (%)	Clay (%)	pH (1:1 w/v
	CB	**+0.075**	**+0.075**	**+0.075**	**+0.077**	0.002	0.022
	BX	**+0.299**	**+0.299**	**+0.299**	**+0.244**	0.054	0.580
	N_{sum}	**+0.350**	**+0.350**	**+0.350**	**+0.291**	**-0.089**	**+0.142**
	NAG	**+0.277**	**+0.277**	**+0.277**	**+0.189**	0.052	0.067
	LAP	**+0.083**	**+0.083**	**+0.083**	**+0.222**	**-0.078**	0.071
	AP	**+0.337**	**+0.337**	**+0.337**	**+0.268**	**-0.101**	0.009

Table S4 : Marginal r^2 values for mixed-effects models with clay concentration, pH, or fungi:bacteria as the sole fixed effect and soil pit as a random effect on EE activities normalized by microbial biomass (MB) or soil organic carbon (SOC) concentration. Key: α-glucosidase (AG), β-glucosidase (BG), cellobiohydrolase (CB), β-xylosidase (BX), N-acetylglucosamine (NAG), leucine aminopeptidase (LAP), and phosphatase (AP). Bolded values represent a significant ($\alpha = 0.05$) effect and +/- signifies the direction of the effect (Clay: n = 143, pH: n = 143, fungi:bacteria: n = 178).

		MB-normalized[1]	*MB-normalized*[1]	*MB-normalized*[1]	*MB-normalized*[1]	*MB-normalized*[1]	*SOC-n*
Enzyme	Enzyme	Enzyme	Clay	Clay	pH	fungi:bacteria	Clay
AG	**+0.144**	**+0.144**	**+0.144**	0.002	0.002	0.007	0.020
BG	**+0.107**	**+0.107**	**+0.107**	0.051	0.051	**+0.100**	< 0.00
CB	**+0.067**	**+0.067**	**+0.067**	0.049	0.049	0.023	0.001
BX	**+0.144**	**+0.144**	**+0.144**	0.017	0.017	**+0.068**	0.001
NAG	**+0.048**	**+0.048**	**+0.048**	0.032	0.032	**+0.099**	0.019
LAP	0.019	0.019	0.019	< 0.001	< 0.001	0.003	**+0.03**
AP	**+0.199**	**+0.199**	**+0.199**	< 0.001	< 0.001	< 0.001	**+0.08**

[1] Enzyme activity g^{-1} microbial biomass

[2] Enzyme activity g^{-1} soil organic carbon

SUPPLEMENTAL FIGURES

Figure S1 : Boxplots showing soil organic carbon (SOC, A), total nitrogen (N, B), Olsen phosphorus (P, C), clay (D), the ratio of fungal to bacterial biomass (E), and pH (F) at each depth interval throughout the top meter of soil across sites. For the boxplots, the solid black line represents the median, and the box represents the interquartile region (IQR). Lines stemming from the boxplots represent 1.5x the IQR and points show data outside of 1.5x the IQR. The blue line shows the best-fit loess regression with standard error highlighted by the gray ribbon.

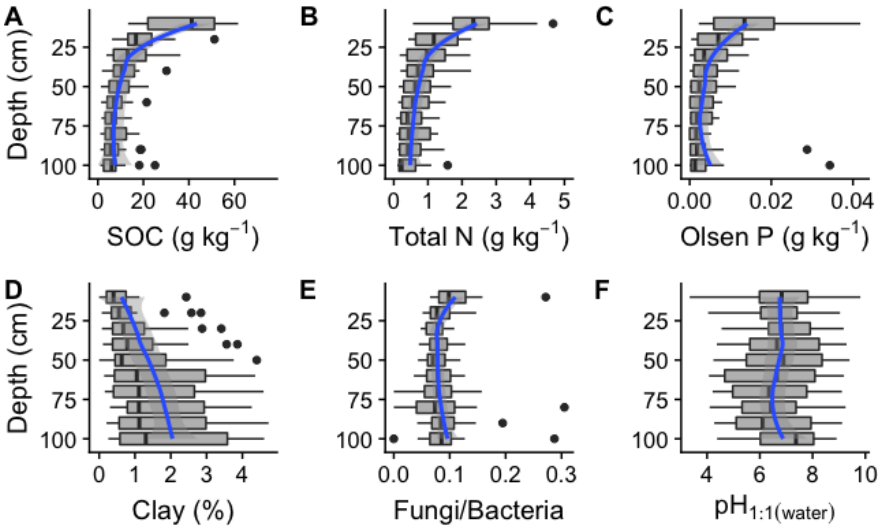

Figure S2 : Potential activity of α-glucosidase (AG), β-glucosidase (BG), β-xylosidase (BX), cellobiohydrolase (CB), N-acetylglucosaminidase (NAG), leucine aminopeptidase (LAP), and acid phosphatase (AP) as a function of depth throughout the top meter of soil across sites. Boxplots show the distribution of extracellular enzyme activities at each depth and the blue line shows the best-fit loess regression with standard error highlighted by the gray ribbon. Note: scale of x-axis differs among extracellular enzymes.

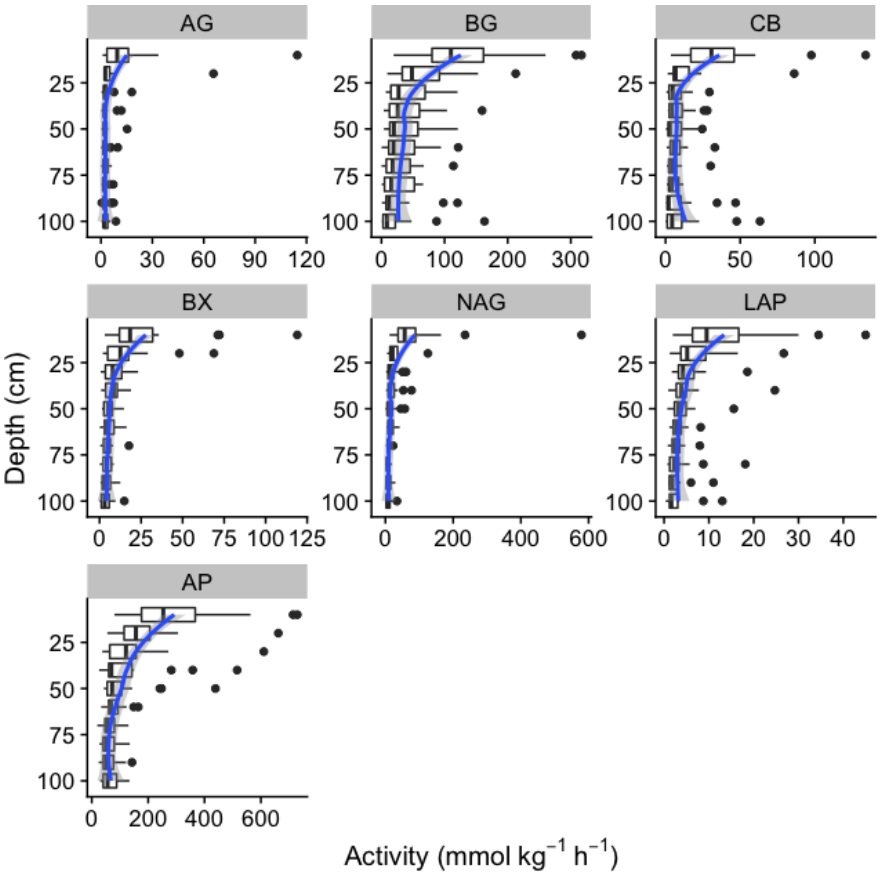

Figure S3 : Potential activity of α-glucosidase (AG), β-glucosidase (BG), β-xylosidase (BX), cellobiohydrolase (CB), N-acetylglucosaminidase (NAG), leucine aminopeptidase (LAP), and acid phosphatase (AP) normalized by soil microbial biomass (mol phospholipid fatty acid [PLFA]) as a function of depth throughout the top meter of soil across sites. Boxplots show the distribution of extracellular enzyme activities at each depth and the blue line shows the best-fit loess regression with standard error highlighted by the gray ribbon. Note: scale of x-axis differs among enzymes.

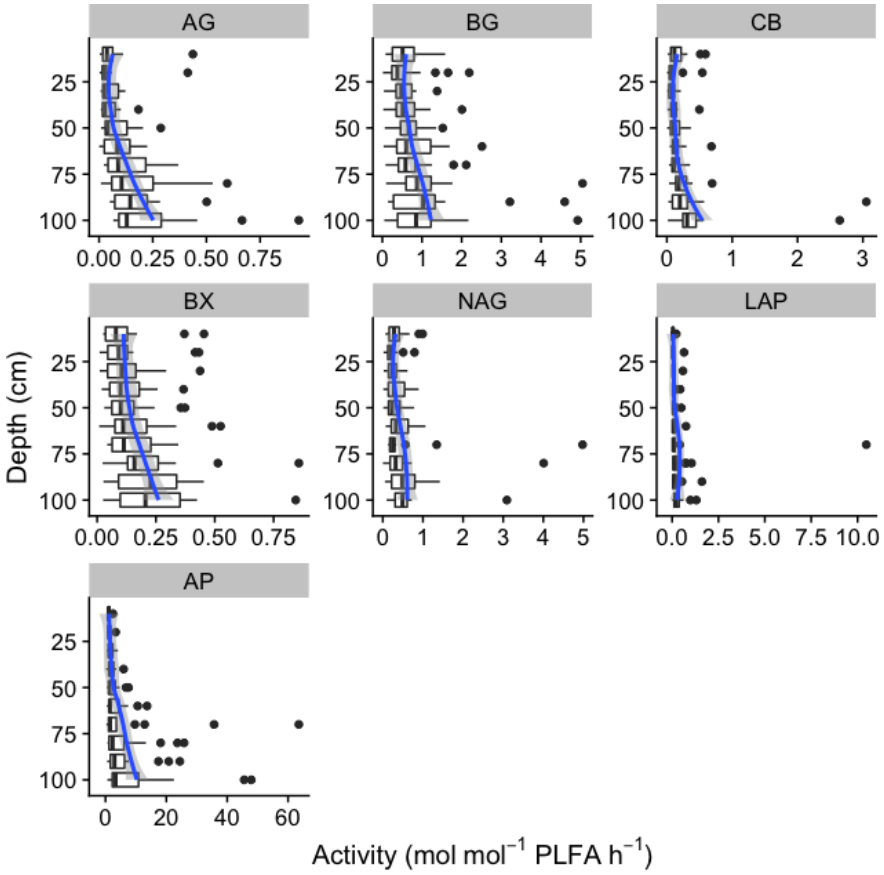

Figure S4 : Proportion of soil microbial biomass-normalized extracellular enzyme activity below 20 cm in the top meter for α-glucosidase (AG), β-glucosidase (BG), cellobiohydrolase (CB), β-xylosidase (BX), N-acetylglucosamine (NAG), leucine aminopeptidase (LAP), and acid phosphatase (AP) across (A) and among (B) soil orders. Error bars show standard error of the mean (Figure panel A: n = 19; Figure panel B: Inceptisol: n = 4, Mollisol: n = 5, Ultisol: n = 3).

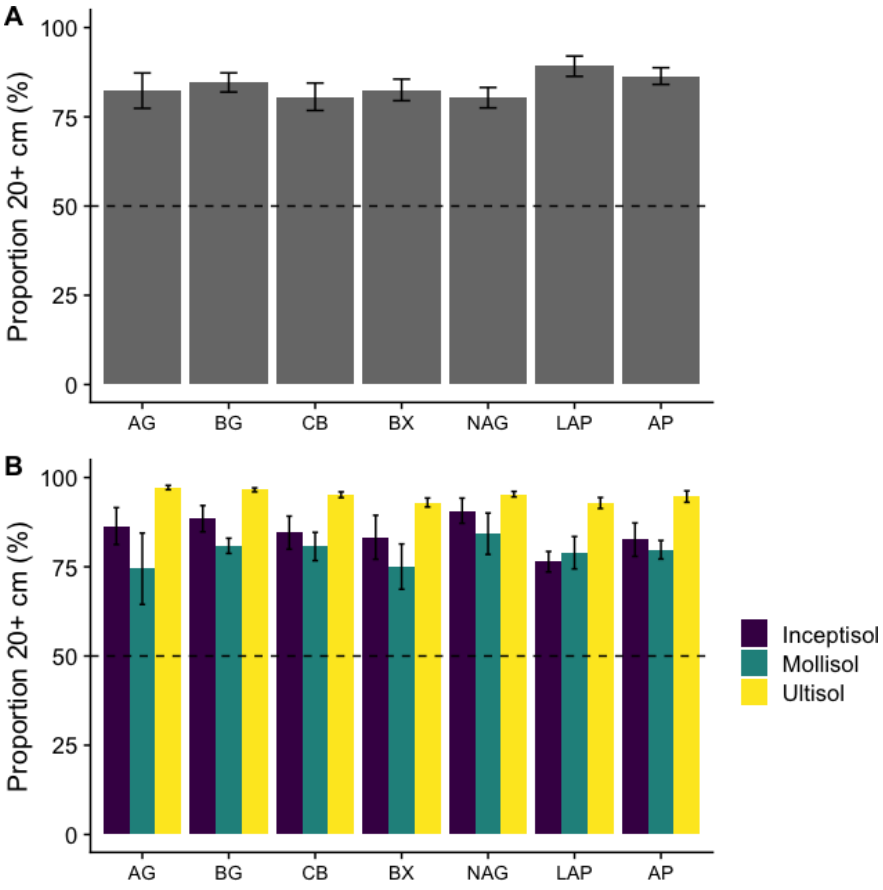

Figure S5 : Potential activity of α-glucosidase (AG), β-glucosidase (BG), β-xylosidase (BX), cellobiohydrolase (CB), N-acetylglucosaminidase (NAG), leucine aminopeptidase (LAP), and acid phosphatase (AP) normalized by kg^{-1} soil organic carbon (C) as a function of depth throughout the top meter of soil across sites. Boxplots show the distribution of extracellular enzyme activities at each depth and the blue line shows the best-fit loess regression with standard error highlighted by the gray ribbon. Note: scale of x-axis differs among enzymes.

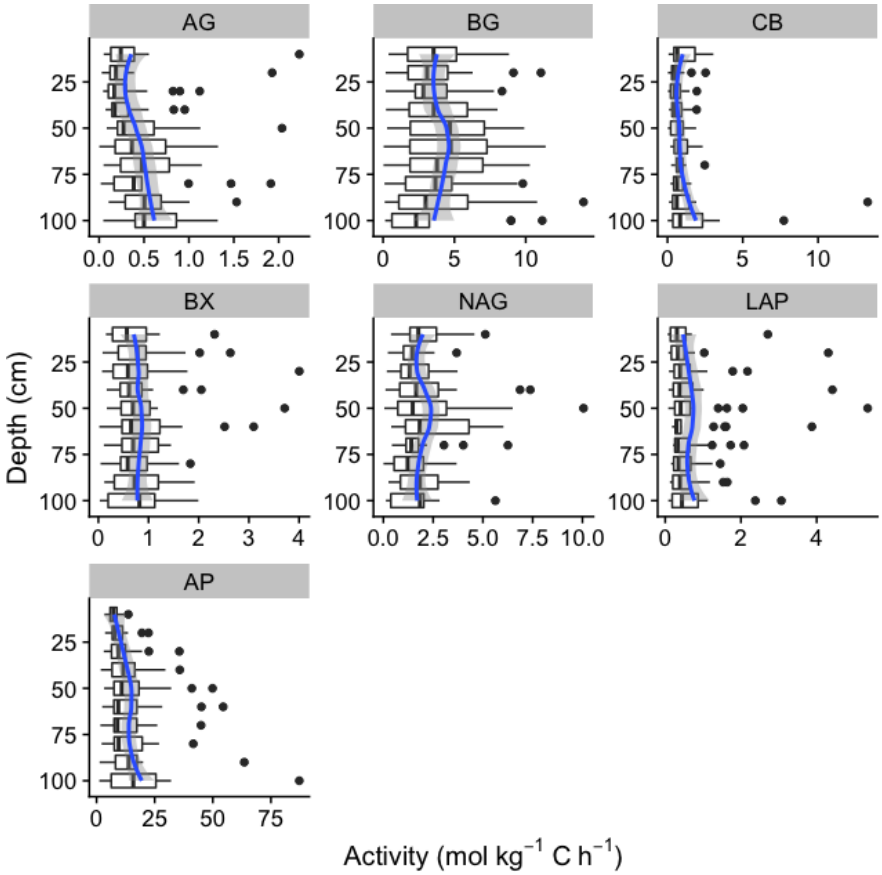

Figure S6 : Proportion of extracellular enzyme activity (kg^{-1} soil organic carbon [C]) below 20 cm in the top meter for α-glucosidase (AG), β-glucosidase (BG), cellobiohydrolase (CB), β-xylosidase (BX), N-acetylglucosamine (NAG), leucine aminopeptidase (LAP), and acid phosphatase (AP) across (A) and among (B) soil orders. Error bars show standard error of the mean (Figure panel A: n = 19; Figure panel B: Inceptisol: n = 4, Mollisol: n = 5, Ultisol: n = 3).

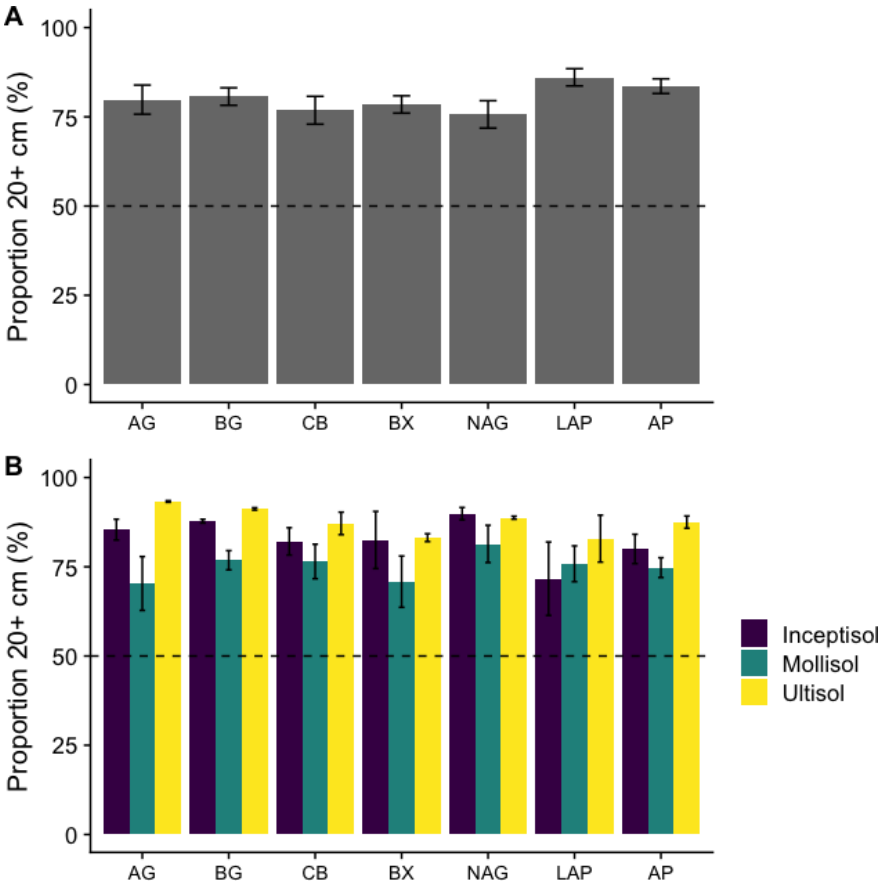

Figure S7 : Lack of relationships between soil and extracellular enzyme (EE) stoichiometry across the whole soil profile. Data points represent individual soil samples (depths within each pit).